

Potential mechanism for response of El Niño–Southern Oscillation variability to change in land surface energy budget

Zeng-Zhen Hu,¹ Edwin K. Schneider,^{1,2} Uma S. Bhatt,³ and Ben P. Kirtman^{1,2}

Received 12 March 2004; revised 26 May 2004; accepted 22 July 2004; published 12 November 2004.

[1] El Niño–Southern Oscillation (ENSO) variability was found to be sensitive to the land surface energy budget from a comparison of two integrations of the coupled general circulation model of Center for Ocean-Land-Atmosphere Studies, a control simulation in which global soil wetness in the three layers is predicted, and a sensitivity experiment in which deep soil moisture is specified. In contrast to the control experiment, in which the net land surface energy flux is zero, the sensitivity experiment leads to land becoming a unphysical and unexpected net energy sink. However, the comparison points toward a physically realizable mechanism by which ENSO can be influenced by changes in land surface properties. The net energy sink causes cooling tropical land surface. The cooling over tropical land is connected with the mean state changes of the coupled system, including a shift in the land/sea partitioning of precipitation toward the oceans, a more westerly wind stress over the tropical Pacific, and a more El Niño-like mean state of the tropical Pacific with a weaker east-west temperature contrast. Meanwhile, sea surface temperature (SST) variance decreases in the central and eastern tropical Pacific, and the ENSO becomes less energetic. A series of diagnostic simulations using an intermediate coupled model tests the impact of the simulated mean state and atmospheric noise changes on the ENSO variability. It is demonstrated that the mean state change plays a key role in determining the ENSO variance change. The mean state change in the sensitivity experiment causes a reduction in the sensitivity of ENSO SST variability to surface wind stress, and is consistent with a decrease in ENSO SST variance. *INDEX TERMS*: 1620 Global Change: Climate dynamics (3309); 3309 Meteorology and Atmospheric Dynamics: Climatology (1620); 3322 Meteorology and Atmospheric Dynamics: Land/atmosphere interactions; 3339 Meteorology and Atmospheric Dynamics: Ocean/atmosphere interactions (0312, 4504); 3374 Meteorology and Atmospheric Dynamics: Tropical meteorology; *KEYWORDS*: El Niño–Southern Oscillation variability, mean state of tropical climate, land surface change, energy budget

Citation: Hu, Z.-Z., E. K. Schneider, U. S. Bhatt, and B. P. Kirtman (2004), Potential mechanism for response of El Niño–Southern Oscillation variability to change in land surface energy budget, *J. Geophys. Res.*, 109, D21113, doi:10.1029/2004JD004771.

1. Introduction

[2] Since the pioneering work of *Charney et al.* [1975], who demonstrated the potential role of vegetation removal in maintaining drought in sub-Saharan Africa and the involved feedbacks between the land surface and the atmosphere, there have been many investigations demonstrating the influence of land-use changes such as deforestation and desertification, and land surface properties such as snow cover and vegetation changes on global and regional climate [*Dickinson and Henderson-Sellers*, 1988; *Barnett et al.*, 1989; *Nobre et al.*, 1991; *Yasunari et al.*, 1991; *Xue and Shukla*, 1993; *Meehl*, 1994; *Zeng and*

Neelin, 1999; *Gedney and Valdes*, 2000; *Zhao and Pitman*, 2002, and references therein]. Climate and land surface conditions are in a dynamic equilibrium in which land surface condition both responds to and affects climate [*Bonan et al.*, 1992]. There is also a significant body of evidence suggesting that soil moisture influences climate change and variability on a wide range of timescales. *Meehl* [1994] shows how soil moisture prior to the monsoon influences subsequent monsoon performance and found that excessive soil moisture cools the land surface, reduces land-sea temperature contrast, affecting surface winds and rainfall. *Shukla and Mintz* [1982] indicated that in the extratropics, the soil with its larger seasonal changes plays a role analogous to that of the ocean. In winter, the ocean heats the atmosphere over it using the energy stored in summer, and in summer the soil humidifies the atmosphere with the precipitation received in winter. Using two atmospheric general circulation model (AGCM) simulations with and without land surface-atmosphere interaction, *Delworth and Manabe* [1988, 1989] found that the interactive soil moisture allows larger variations of surface

¹Center for Ocean-Land-Atmosphere Studies, Calverton, Maryland, USA.

²Also at George Mason University, Fairfax, Virginia, USA.

³International Arctic Research Center, Frontier Research System for Global Change, University of Alaska Fairbanks, Fairbanks, Alaska, USA.

energy fluxes, thereby increasing the variance of surface air temperature.

[3] The influence of land surface processes on ocean variation is also evidenced in a few investigations. For example, *Barnett et al.* [1989] and *Meehl* [1997] both show that a colder land surface over Asia is associated with anomalous westerly surface winds over the Pacific that affect ENSO. *Zhang et al.* [1996] found that modification of model surface parameters to simulate tropical deforestation produces significant modifications of both Hadley and Walker circulations. *Zeng et al.* [1996] showed the possible impact of Amazon deforestation on SST change across the Atlantic ocean and in the eastern equatorial Pacific in an intermediate model. *Bhatt et al.* [2003] described a connection found between land-atmosphere coupling and midlatitude SST variability in the North American–North Atlantic sector. They found that specifying soil moisture results in a reduction of the SST variance in the midlatitude Atlantic. The far-field response of ocean, for example, the El Niño–Southern Oscillation (ENSO), to land surface processes and change is receiving increased research interest. In this work, a potential mechanism for response of ENSO variability to change in land surface energy budget was suggested from a comparison of two integrations of the Center of Ocean–Land–Atmosphere Studies (COLA) coupled general circulation model (CGCM), one with and one without interactive soil moisture. In section 2, the coupled model, experimental design, and data are briefly described. The influence of specified soil moisture on energy budget and the possible associated feedbacks are analyzed in section 3. The simulated mean state and ENSO variability in the two experiments are compared in sections 4 and 5, respectively. The possible mechanism is investigated in section 6. Section 7 contains summary and discussion.

2. Model Description and Experiment Design

[4] The COLA CGCM is composed of the COLA AGCM and the Geophysical Fluid Dynamics Laboratory MOM2 oceanic GCM (OGCM). The COLA AGCM is run at T30 (4° latitudes \times 5° longitudes) grid resolution with 18 sigma levels in the vertical. The OGCM has 20 levels in the vertical and a longitudinal grid resolution of 3° , and a latitudinal resolution of 3° poleward of 30° , which reduces to 1° within 10° of the equator. The AGCM and OGCM are coupled once per day without any flux correction. Details of the coupled model and its ability to simulate present-day climate and its variability are shown in the work of *Schneider and Kinter* [1994], *DeWitt and Schneider* [1999, 2000], *Wajsowicz and Schneider* [2001], *Schneider* [2001], and *Bhatt et al.* [2003]. The results of two intercomparison projects, the El Niño Simulation Intercomparison Project (ENSIP; *Latif et al.* [2001]) and the Study of Tropical Oceans in Coupled Models (STOIC; *Davey et al.* [2002]), show that the COLA CGCM is one of the best models in simulating the tropical mean state and variability.

[5] The land surface scheme coupled to the AGCM is a version of the simplified Simple Biosphere (SiB) model of *Sellers et al.* [1986] that is described by *Xue et al.* [1991], and referred as SSiB. The soil moisture is simulated in three layers: a thin surface layer (2 cm), a root layer that varies in depth according to vegetation types (0.2–1.5 m), and a deep

recharge zone (0.3–2.0 m). In SSiB, the vegetation is modeled explicitly, and controls on water uptake and transpiration are governed by moisture potentials and water and temperature stress thresholds [*Xue et al.*, 1996]. The version used in the experiments is modified to allow the user to specify the independent two-dimensional grids of soil properties, and two-dimensional seasonally varying grids of vegetation cover fraction, greenness, and leaf area index [*Dirmeyer and Zeng*, 1997].

[6] The potential for the influence of the land surface process modifications on ENSO variability is examined using two integrations of the COLA CGCM. In the control experiment, of 190 years duration, global soil wetness in the three layers is predicted, thereby including the full interaction between soil wetness and atmosphere/ocean. This is a fully coupled experiment, referred to as COU. In the sensitivity experiment, of 82 years duration, the seasonal cycle of global soil wetness at the two lower layers is specified at each grid point based on a 20 year average of the first experiment during the years 87–106 of its 190 year integration, but the soil wetness at the surface layer is predicted as in COU. The second integration is referred to as OCN. Since both experiments employ the same dynamical ocean and atmosphere, the differences in atmospheric and oceanic variability between the two integrations are due only to the modification of the land component model. In order to do this comparison, only the common 82 years of data of the two experiments are used in this work. Details of the experiments are given in the work of *Bhatt et al.* [2003].

[7] The simulated variables used in this study include monthly mean temperature, geopotential height, sea level pressure (SLP), total precipitation, cloud cover, soil wetness, zonal component of wind fields, surface wind stress, energy budget, vertical velocity in the ocean averaged for the upper 60 m, subsurface ocean temperature, and oceanic heat content of vertically averaged temperature for the upper 250 m. To examine the reality of simulated mean surface temperature, monthly mean temperature at 2 m is used, which is derived from the reanalysis of the National Center for Environmental Prediction and National Center for Atmospheric Research [*Kalnay et al.*, 1996]. The reanalysis data span the period of January 1948 to December 2002 with a $1.875^\circ \times 1.875^\circ$ horizontal resolution. The discussion is concentrated on the tropics and focused on the comparison of interannual variabilities and mean state changes in the two experiments, OCN and COU. All the figures and calculations are made using monthly (from January to December) data.

3. Energy Budget and Feedback Processes

[8] Figure 1a displays OCN-COU surface energy budget analysis. A negative difference means heat being pulled from the surface into the atmosphere, and a positive difference means heat being put into the surface, so the convention is positive downward. The largest differences of the surface energy budget between OCN and COU are -8 W/m^2 over tropical land, and 6 W/m^2 over the eastern tropical Pacific (Figure 1a). The amplitudes of these differences are less than 10% of the total surface energy budget over the eastern tropical Pacific. The surface energy budget differences between the two experiments come from some

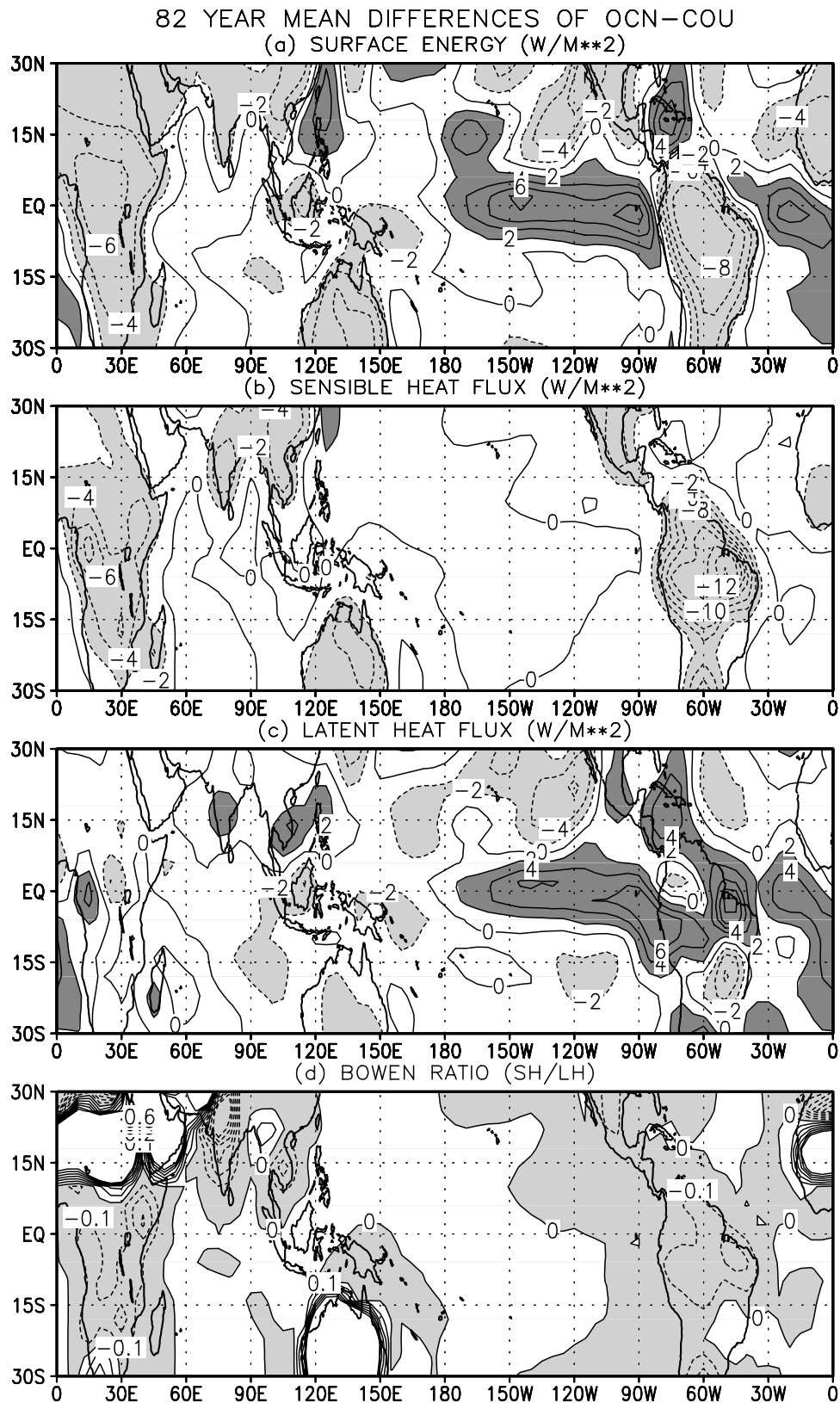


Figure 1. (a) Differences (OCN–COU) in surface energy budget, (b) sensible heat flux, (c) latent heat flux, and (d) Bowen ratios. Positive values indicate a flux out of the surface, and contour interval is 2 W/m^2 in Figures 1a–1c. The shaded regions show differences greater than 2 W/m^2 or less than -2 W/m^2 in Figures 1a–1c, and less than 0.0 in Figure 1d. This figure and all the following figures are made with monthly (January to December) data.

unexpected features, since the long-term annual mean of the net surface energy flux should be close to zero over land. As the net energy flux into land is close to zero in COU, the differences is due mostly to land becoming a net energy sink in OCN. The globally and annually averaged net surface radiative flux is -2.9 W/m^2 in COU and -3.6 W/m^2 in OCN.

[9] The energy sink over the tropical land area is unphysical and unexpected. Since the surface energy in the control run (COU) is generally balanced, it is very likely that the imbalance occurred after the original model was revised for the sensitivity experiment. When simulated energy or water components in the model soil layer are replaced by specified ones, energy and mass are added or subtracted from existing soil layers, naturally causing the energy imbalance at the land surface unless additional energy terms are added in the surface energy balance equation to reflect such modification. Just as in specified SST experiment, if we specify the SST by an observed one, the ocean energy will not be balanced in the model. The large heat capacity and ocean current are the main reason caused the surface energy budget differences in the oceans. We believe, however, that further analysis offers the opportunity to understand the mechanism by which land surface energy imbalance in the model and land use changes in the real climate system could influence ENSO and the mean state. The analysis in the next section puts forward a plausible mechanism.

[10] The net energy loss into the land is associated with a reduction of upward sensible heat flux (Figure 1b). Positive values of latent heat flux over the eastern tropical Pacific dominate the net energy gain from the ocean (Figure 1c). The differences (OCN-COU) of the net longwave radiation at bottom are almost in balance with the differences of shortwave radiation absorbed at the ground (not shown). Thus the radiative fluxes make a small contribution to the total surface energy budget differences. It is the difference in the Bowen ratio over land (Figure 1d) that really causes the changes in atmospheric circulation and ocean currents. The Bowen ratio difference shows the change of the partition of available energy between sensible and latent heat. The specified soil moisture, which is based on climatology, produces a different ratio of latent to sensible heat flux, which alters atmospheric circulation and ocean circulation. However, the Bowen ratio difference in this experiment is associated with the model design, which did not conserve the surface energy balance at the land surface. This may affect the feedback of land surface to the changes in ocean current, which is initially caused by specifying soil moisture.

[11] The feedback processes play a secondary role in the surface energy imbalance. For example, fixing the deep soil moisture in OCN can be thought of as providing an infinite source of water and could lead to changes in some feedback processes. One of the affected feedbacks is the latent heat, cloud cover, radiation, and surface temperature feedback. Through a comparison of the two experiments, we found that fixing the deep soil moisture led to increased soil wetness at the surface zone (Figure 2a) and increased clouds (Figure 2b), which reduces the downward shortwave radiation at ground (Figure 2c) and at top of the atmosphere (Figure 2d), then reinforces the lower temperatures. That is consistent with lower surface temperature, less sensible heat

flux, and energy sink over land shown in OCN. This is an indication that the model's performance in OCN is physically reasonable.

[12] There may be other factors contributing to the cold land surface. For instance, through an increase in latent heat fluxes (Figure 1c), the constrained soil water in OCN leads to a moisture source with associated cooling. In addition, the drastically cooling over land surface (Figure 3a) pulls heat out of the land surface, thus giving negative sensible heat flux differences (Figure 1b). Indeed, the detailed influence of constraining soil moisture on feedback processes is quite complicated.

[13] Comparing with the reanalysis data shows that simulated mean surface temperature patterns in OCN and COU are reasonable well over tropical land and oceans (figures not shown). The simulated surface temperature in OCN and COU is $1\text{--}4^\circ$ warmer over tropical land than in the reanalysis. The largest warming is along the eastern coast of South America. The realistic simulations of the mean surface temperature benefit the credibility of following sensitivity analyses.

4. Shift in the Mean State

[14] The surface energy budget changes cause the mean state change over tropical land and oceans. It is found that the differences of the mean surface temperature between OCN and COU are large (Figure 3a). The SST is 0.3°C warmer in OCN than in COU in the eastern tropical Pacific. SST changes are negative in the western tropical Pacific. The distribution pattern of SST difference in Figure 3a bears some similarities to the SSTA pattern in the developing phase of an El Niño event [Rasmusson and Carpenter, 1982]. Warming over the Atlantic Ocean is also evident. Surface temperature change over land is much more remarkable than that over the oceans. Cooling dominates over all continents with amplitudes of 0.5° to 1.5°C . The surface temperature changes are consistent with the vertical and horizontal cross-section distributions of temperature differences along the equator averaged in the latitudinal bands from 5°S and 5°N shown in Figure 4a. Cooling in upper troposphere is also noticeable (Figure 4a).

[15] Differences in precipitation and SLP are closely related to the surface temperature change. Positive (negative) surface temperature anomalies (Figure 3a) generally correspond to above (below) normal precipitation (Figure 3b). The SLP change favors the negative phase of the Southern Oscillation (SO) (Figure 3c) that is consistent with above normal precipitation in the eastern tropical Pacific (Figure 3b). Warming in the lower troposphere and cooling in the upper troposphere over the eastern tropical Pacific and tropical Atlantic (Figure 4a) reinforces the instability that favors the enhanced precipitation in those regions in OCN (Figure 3b). Thus the warming over the oceans and cooling over the continents shift the land/sea partition of precipitation toward the oceans, especially near South America.

[16] The surface heat flux changes cause wind and divergence changes (Figures 4b, 4c, and 5a). The cooling over the American continent and warming in the tropical eastern Pacific and tropical Atlantic (Figures 3a and 4a) lead to convergence at lower levels and divergence at higher

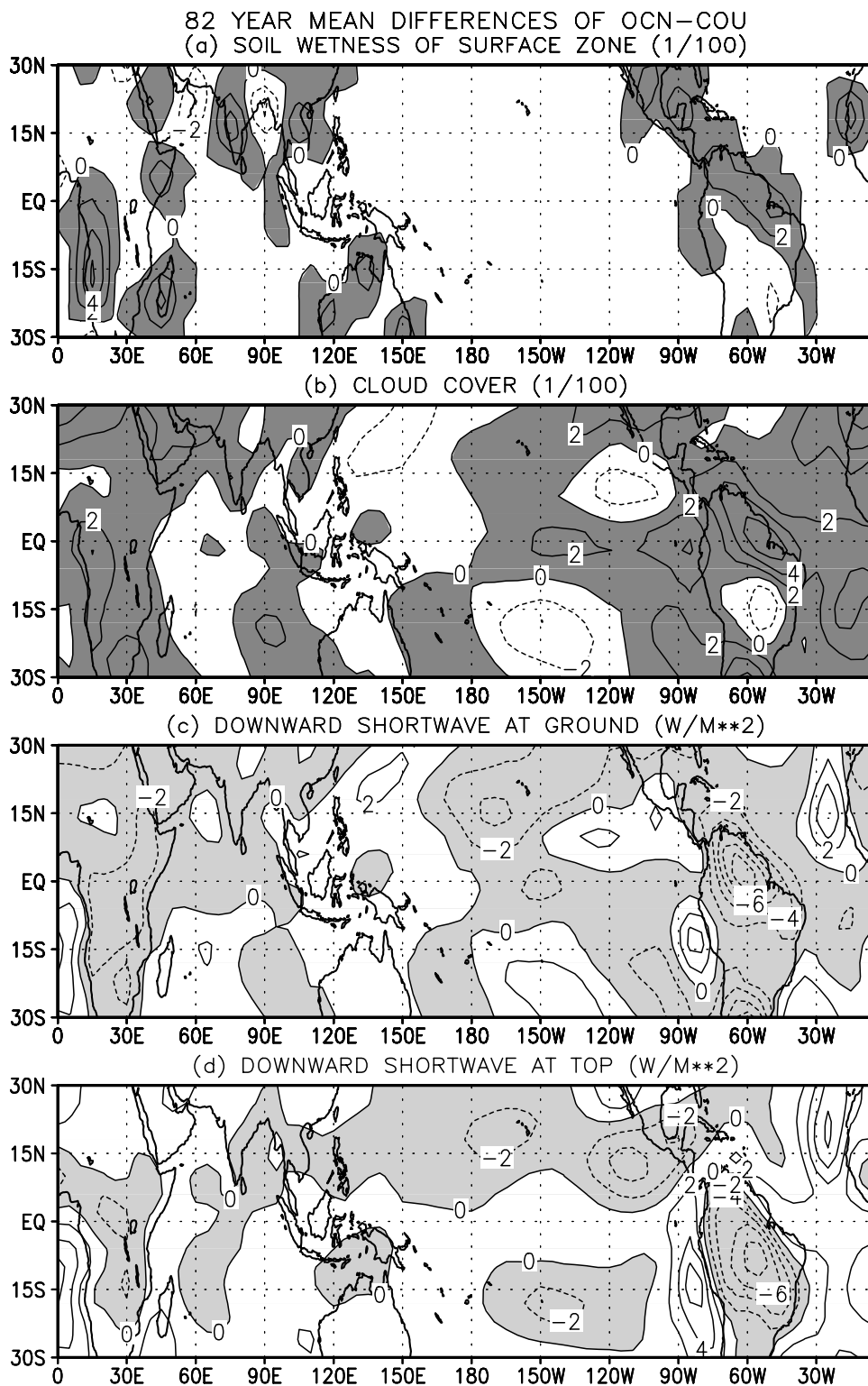


Figure 2. Differences (OCN-COU) in (a) soil wetness, (b) cloud cover, (c) downward shortwave radiation at ground, and (d) at the top of the atmosphere. Contour interval is 0.02 in Figures 2a and 2b, and 2 W/m² in Figures 2c and 2d. The shaded regions show positive differences in Figures 2a and 2b, and negative differences in Figures 2c and 2d.

levels in the tropical eastern Pacific and tropical Atlantic (Figures 4c and 5a), that are associated with the shift of the land/sea partition of precipitation toward the oceans (Figure 3b). The convergence of oceanic surface wind stress

results in downwelling in the tropical central and eastern Pacific (Figure 5b) and a deepening (shallowing) of the thermocline in the tropical eastern (western) Pacific (Figure 5c). Subsurface ocean temperature change along

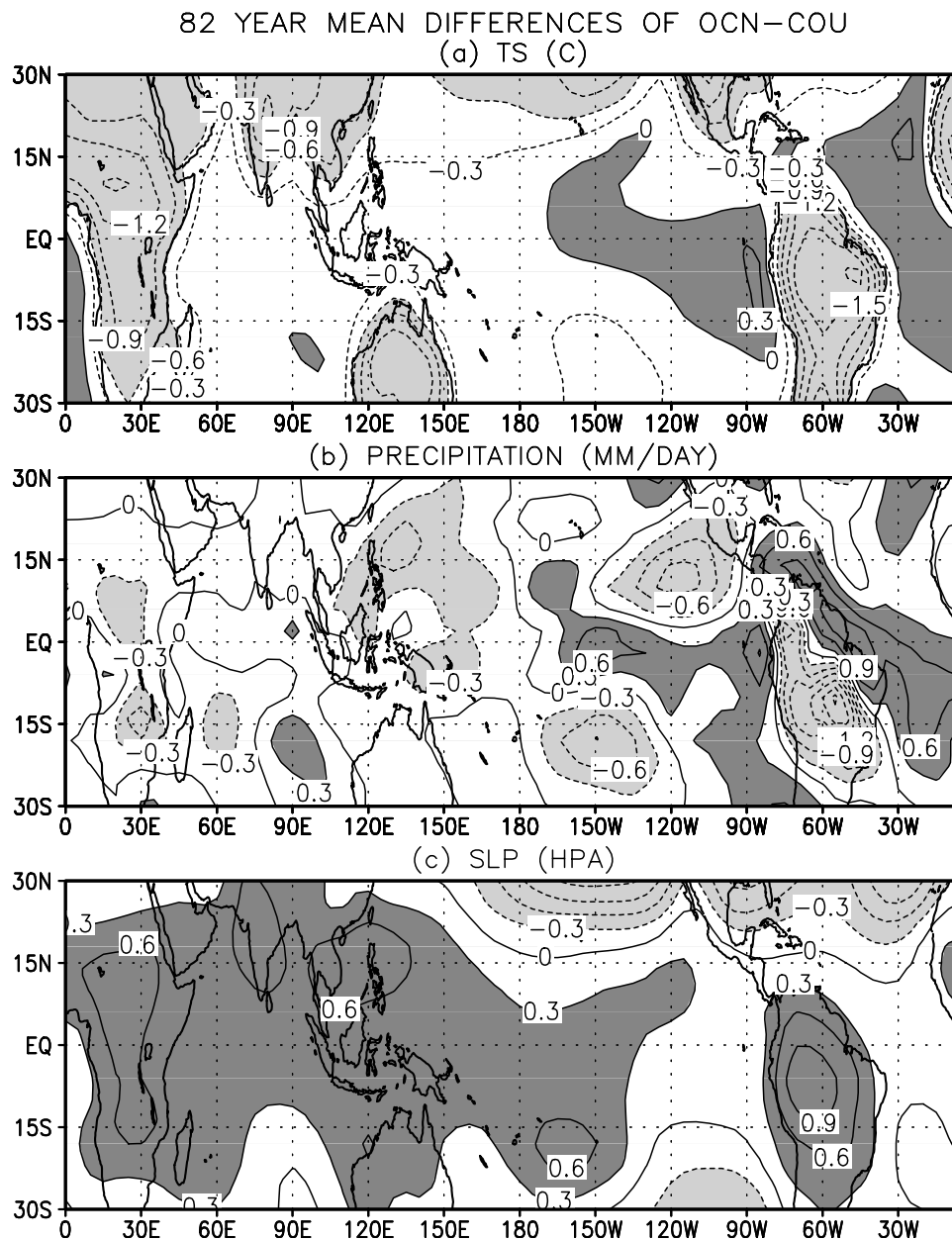


Figure 3. (a) Differences (OCN–COU) in mean surface temperature (TS and SST), (b) precipitation, (c) and sea level pressure in the tropics and subtropics. Contours are 0.3°C in Figure 3a, 0.3 mm/day in Figure 3b, and 0.3 hPa in Figure 3c. The shaded regions represent the SSTA greater than 0.0°C or less than -0.6°C in Figure 3a, greater than 0.3 mm/day or less than -0.3 mm/day in Figure 3b, and greater than 0.3 hPa or less than -0.3 hPa in Figure 3c.

equator is a cooling in the west and warming in the east (Figure 6). The subsurface ocean temperature change pattern in Figure 6 is similar to the result of *Arblaster et al.* [2002, Figure 8]. These changes in the ocean are consequences of the cooled land surface that resulted from the heat loss in the sensitivity experiment.

5. Changes of ENSO Variability

[17] The above results demonstrate a significant change of the tropical Pacific mean state. As a consequence, ENSO variability is expected to change in the sensitivity experi-

ment. Figure 7 presents the time series of the Niño3 index for raw data (Figure 7a) and 1–20 year band-pass filter data (Figure 7c), and the corresponding occurrence frequency distributions (OFD) (Figures 7b and 7d). The index is defined as the anomaly of monthly mean SST averaged in $5^{\circ}\text{S}–5^{\circ}\text{N}$, $150^{\circ}\text{W}–90^{\circ}\text{W}$. The correlations between the Niño3 index and SST and sea level pressure (SLP) (not shown) demonstrates that both simulations capture the basic spatial feature of ENSO related variability. We apply a 1–20 year band-pass filter [Press et al., 1992] to the monthly mean time series of the Niño3 index in order to isolate the ENSO variability from long term (longer than 20 years) and

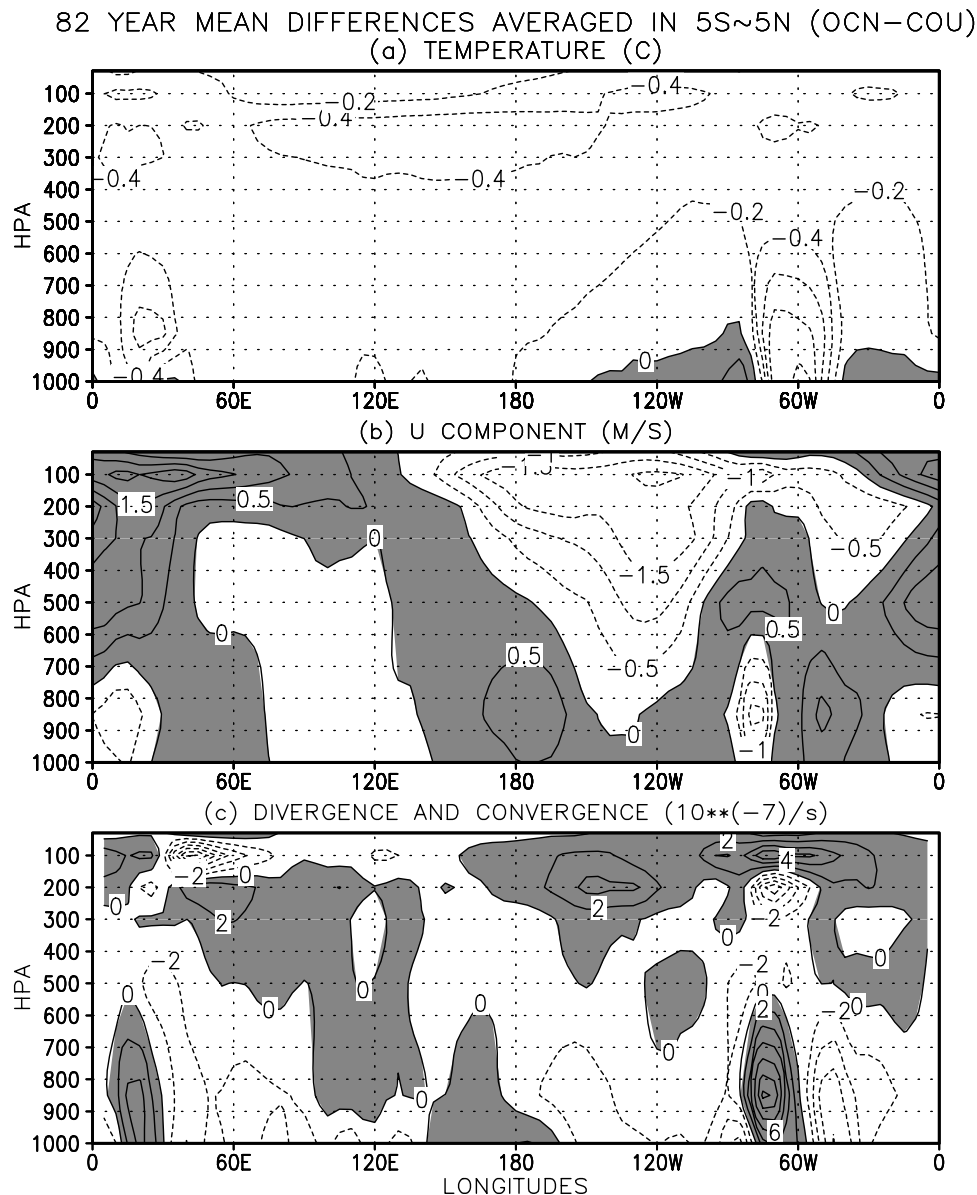


Figure 4. (a) Vertical view of temperature, (b) zonal wind (u), and (c) divergence and convergence differences (OCN-COU) averaged between 5°S and 5°N . A factor of 10^7 is used in Figure 3c for readability. Contour intervals are 0.2°C in Figure 4a, 0.5 m/s in Figure 4b, and $2 \times 10^{-7}\text{ s}^{-1}$ in Figure 4c. The shaded regions represent positive values.

short-term (shorter than 1 year) variations in the simulations. The band-pass filter results (Figure 7c) reduce the amplitudes of the Niño3 index.

[18] The ENSO variance decreases clearly in the sensitivity experiment. The variances of monthly Niño3 SST index of OCN are $0.201\text{ }(^{\circ}\text{C})^2$ for the raw data and $0.147\text{ }(^{\circ}\text{C})^2$ for the band-pass filter data. The corresponding values for COU are $0.312\text{ }(^{\circ}\text{C})^2$ and $0.220\text{ }(^{\circ}\text{C})^2$. The ratio of the Niño3 SST variances of OCN to COU is 0.64 for the raw data and 0.67 for the band-pass filter data. The ratios are significant at the level of 99.9% using an F test, which indicates that the differences of the ENSO variability between the two experiments are statistically significant.

[19] The influence of the land surface cooling on the variances or on the relationship between the amplitude and

occurrence frequency of the Niño3 index can also be examined through comparing the OFD in the experiments. For both raw data and band-pass filter data (Figures 7b and 7d), the values of OFD in OCN are greater than that in COU for SST anomalies (SSTA) with smaller amplitudes, and less than that in COU for SSTA with larger amplitudes. The OFD differences in Figure 7 demonstrate that the tropical land cooling causes a reduction of large (or enhancement of small) amplitude anomalies of the Niño3 index. That signifies that OCN favors the reduction of variability of the Niño3 index in comparison with COU. In addition, the influence of the land surface cooling on the ENSO variability displays a weak seasonality. The influence is slightly larger in winter and summer than in spring and autumn (not shown). The ratios of the Niño3 SST variances of OCN to

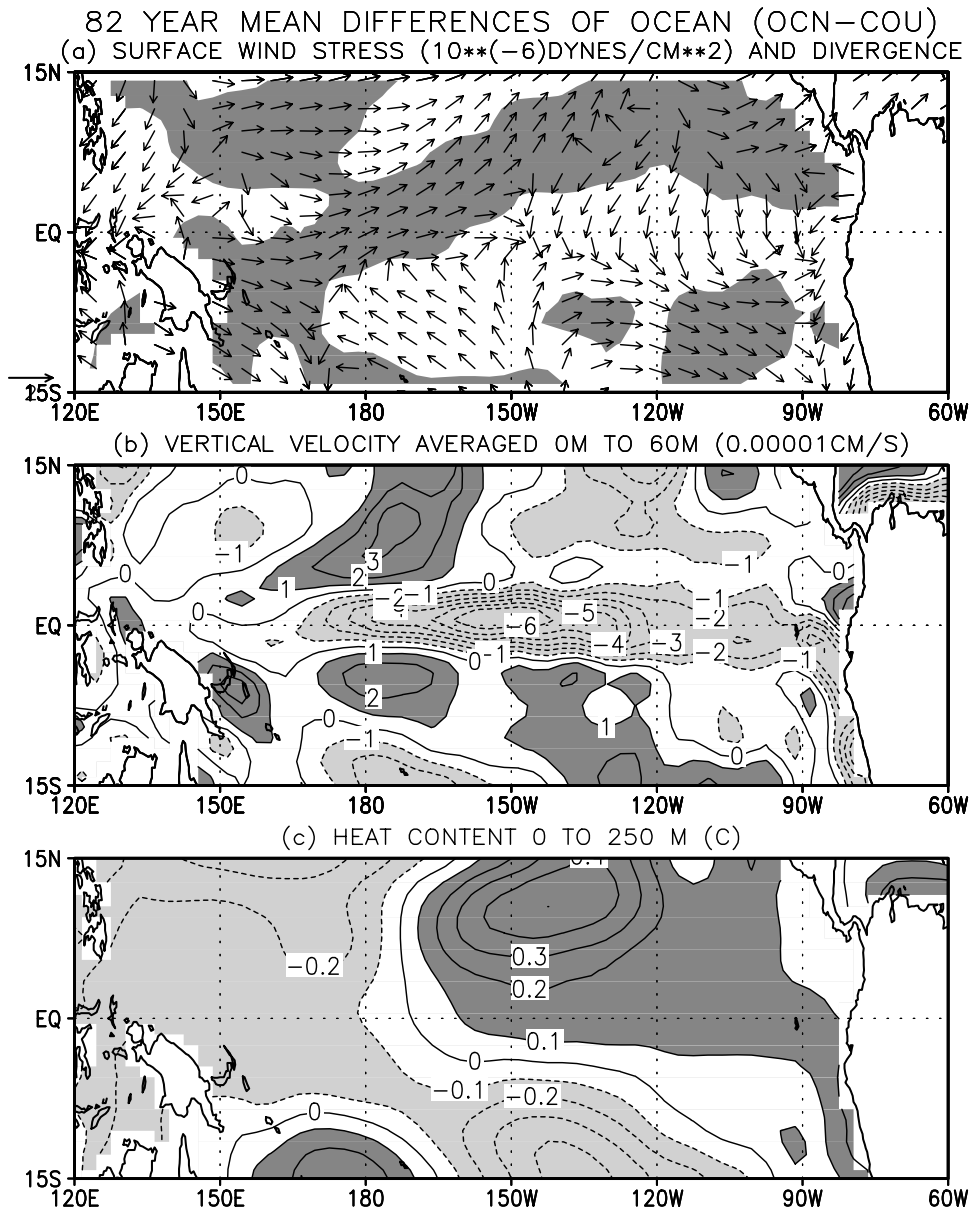


Figure 5. (a) Differences (OCN–COU) of oceanic surface wind stress and divergence, (b) oceanic vertical velocity (average of upper 60 m), (c) and ocean heat content (averaged temperature over upper 250 m) in the tropical Pacific. A factor of 10^5 is used in Figure 5b with contour interval of 1.0×10^{-5} cm/s. The contour interval is 0.1°C in Figure 5c. The shaded regions represent divergence in Figure 5a, absolute differences greater than 1.0×10^{-5} cm/s in Figure 5b and greater than 0.1°C in Figure 5c.

COU for seasonal mean data are 0.69 for winter, 0.76 for spring, 0.70 for summer, and 0.73 for autumn. All these ratios are significant at the 99.9% significance level using an F test.

[20] The variance change of the Niño3 index is confirmed by the two-dimensional distribution of the ratios of surface temperature variances of OCN and COU for the raw data (Figure 8a), 1–20 year band-pass filter data (Figure 8b), and 1 year high-pass filter data (Figure 8c) in the tropical Pacific. The general feature of the ratio distribution in Figure 8 is the variance decrease in the tropical Pacific. The significantly reduced variances in OCN are mainly located in the central and eastern tropical Pacific with factors of 0.6 to 0.8 for the raw data (Figure 8a) and the

band-pass filter data (Figure 8b), and less than 0.8 for the high-pass filter data (Figure 8c). The most significant decrease of the variances in OCN is over the eastern Pacific and South America (180 to 70W). The variance decrease is more obvious over land, which shows the direct influence of the land surface cooling. Some other variables, including cloud cover, geopotential height at 500 hPa, SLP (not shown), and surface wind stress (Figure 9) present similar variance changes. The conclusion that ENSO is suppressed due to the land surface cooling is complementary to the results of *Bhatt et al.* [2003], who found a reduction in surface and atmospheric temperature variability in North America, and in SST variability in the midlatitude Atlantic in the sensitivity experiment.

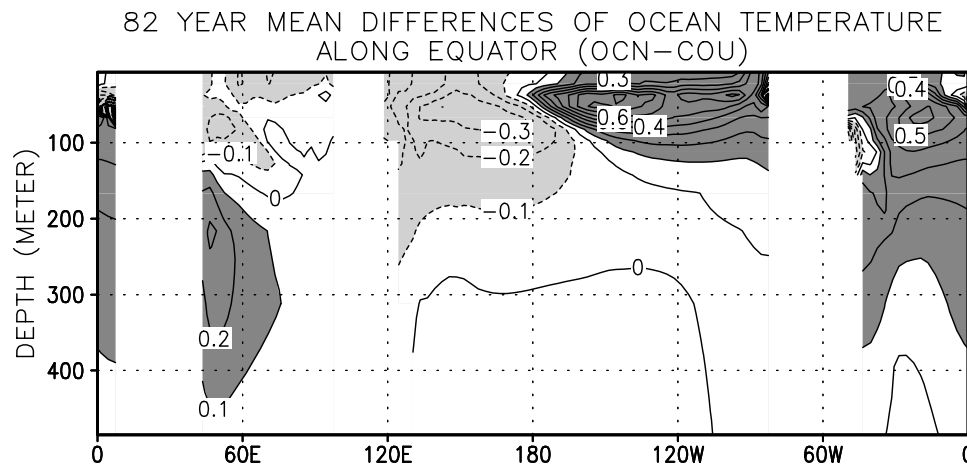


Figure 6. Differences (OCN-COU) of ocean temperature along equator. The contour interval is 0.1°C . The shaded regions represent absolute differences greater than 0.1°C .

[21] Power spectra analyses of the Niño3 index show no significant difference in the dominant frequencies, which are 2.5–5 years, between OCN and COU (not shown). It seems that the effect of the tropical land cooling in the sensitivity experiments is mainly to reduce the amplitudes of ENSO variability and not to change its frequencies.

6. Analysis of the Mechanism for the Change in ENSO Variability

[22] The surface energy loss cools the land surface, and the net energy gain makes the eastern tropical Pacific warmer. At this point, one could ascribe the changes in ENSO variability and the mean state of tropical climate to an unexpected energy budget difference over land. It is clear that tropical land cooling and associated atmosphere coupling and/or the alteration of the mean state of the coupled model reduce the amplitude of the surface temperature variability over both the ocean and land. Given the changes in the land-atmosphere coupling in the OCN experiment, the reduction in the land surface temperature variability was expected. Current scientific understanding of ENSO dynamics suggests two possibilities for the reduced SST variability: (1) the reduced variability over land leads to reduced stochastic “atmospheric noise” in the tropical Pacific, which in turn reduces the amplitude of the ENSO events and (2) changes in mean state alter the coupling in such a way as to reduce the amplitude of the ENSO events.

6.1. Atmospheric Noise

[23] The impact of stochastic atmosphere noise on ENSO variability has received considerable attention in the literature. *Kleeman and Power* [1994] and *Kleeman and Moore* [1997] argued that a major fundamental limitation on the predictability of the ENSO is provided by the stochastic nature of the forcing of the tropical coupled ocean-atmosphere system by atmospheric transients. *Flügel and Chang* [1996] indicated that stochastic forcing has a considerably larger impact on ENSO predictions at short lead times (up to about nine months) than the nonlinear dynamics. *Thompson and Battisti* [2001] showed that the structure and temporal properties of the simulated ENSO are

insensitive to the details of the prescribed stochastic forcing. *Kirtman and Shukla* [2002] examined the role of noise in the framework of an anomaly coupled GCM using a new coupling strategy referred to as an “interactive ensemble.” The main idea behind the “interactive ensemble” is to reduce the atmospheric noise, and thus, examine its impact on climate variability. They found that irregularity of ENSO is due to atmospheric noise, but the fundamental oscillation is self-sustained. Conversely, *Zebiak* [1989] argues that the intraseasonal variability is not an essential component of ENSO. With the *Zebiak and Cane* [1987] model, and an idealized representation of intraseasonal forcing, *Zebiak* [1989] found that the intraseasonal variability generally plays a minor role in altering the model behavior. Recently, *Chen et al.* [2004] shows the intraseasonal variability may not be overwhelmingly important in affecting the ENSO predictability.

[24] In order to test the noise hypothesis, we calculated the ratios of variances of the u component of surface wind stress of OCN and COU for the raw data (Figure 9a), 1–20 year band-pass filter data (Figure 9b), and 1 year high-pass filter data (Figure 9c). The decrease of the variance in OCN is clear for the band-pass filter data and the high-pass filter data, especially over the continents, which results from the suppression of local land-atmosphere interaction and is consistent with Figure 8. It is also noticeable for the exist of the variance increase in the southern Indian and southern Pacific Oceans. Supposing that the 1 year high-pass filtered data represent atmospheric noise, the noise is obviously smaller in OCN than in COU over land and also in most regions of the tropical Pacific (Figure 9c).

[25] The influence of different amplitudes of the atmospheric noise on SST variability is examined by putting the time series of high-pass filtered wind stress of OCN and COU into an intermediate coupled ocean-atmosphere model. The model consists of a very simple statistical atmosphere coupled to the ocean model used in the *Zebiak and Cane* [1987] coupled model. The model used in this work is the same model used in *Kirtman and Schopf* [1998], and its behavior in extended integrations is documented in the work of *Kirtman* [1997]. Details of the modified coupled model are introduced in the work of *Kirtman*

MONTHLY NINO3 (5S~5N,150W~90W) SSTA & FREQUENCY DISTRIBUTION

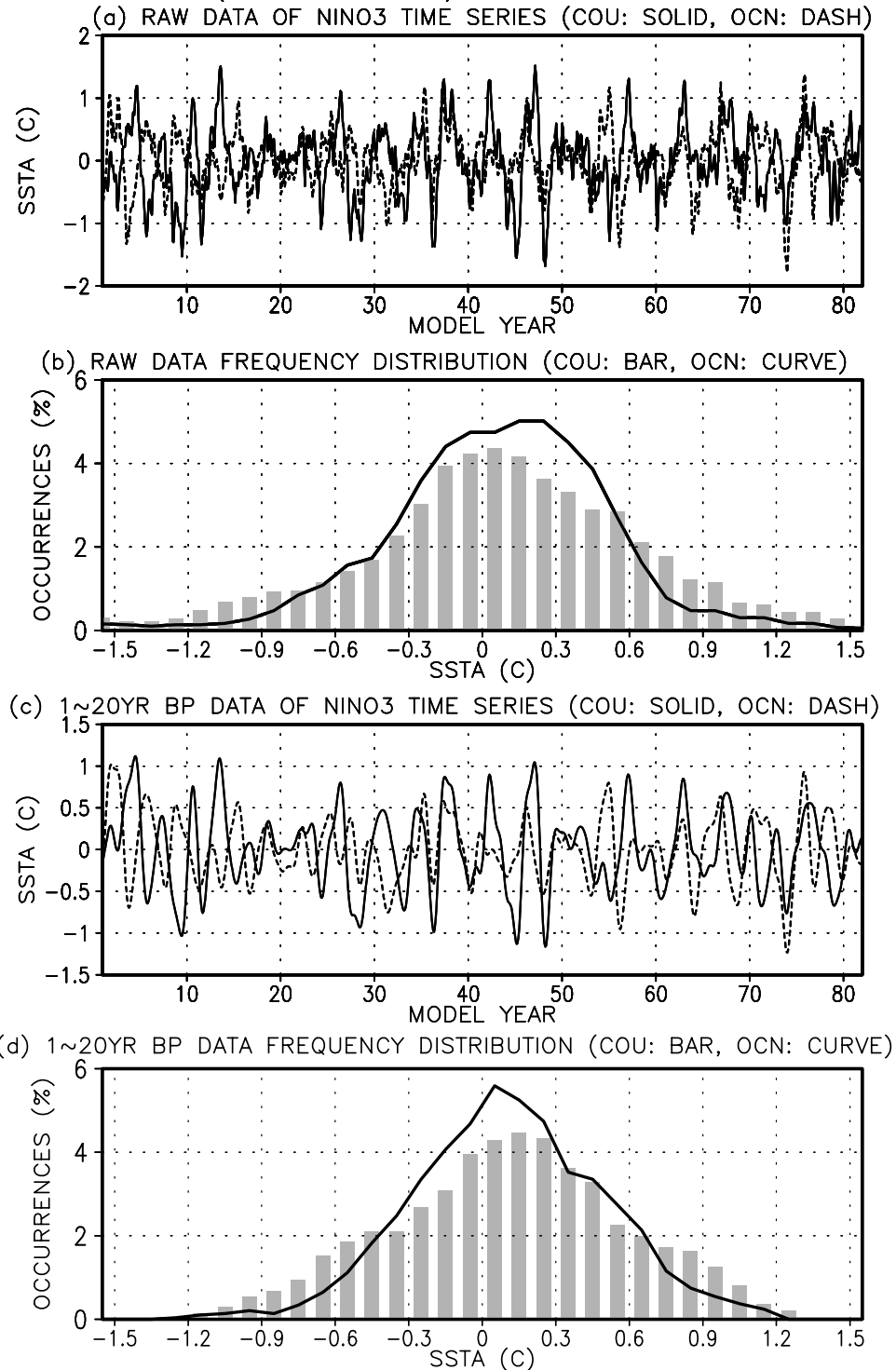


Figure 7. (a and c) Niño3 time series of monthly mean SSTA averaged over 5°S – 5°N , 150°W – 90°W for raw data and 1–20 year band-pass filter data and (b and d) the corresponding frequency distributions. The solid (dashed) curves in Figures 7a and 7c are COU (OCN), and the bars (curves) in Figures 7b and 7d are the corresponding frequency distributions.

[1997] and Kirtman and Schopf [1998]. The simple coupled model experiments presented here are integrated for 82 years, corresponding to the data analyzed from the COU and OCN simulations. Figure 10 displays the ratios of the simulated SST variances of OCN divided by that of

COU. The variance reduction is clear in the western Pacific and eastern subtropical Pacific, but the reduction is minor in the tropical eastern Pacific. This suggests that the amplitude change of the atmospheric noise does not play a key role in the SST variance change. However, a caveat is that the

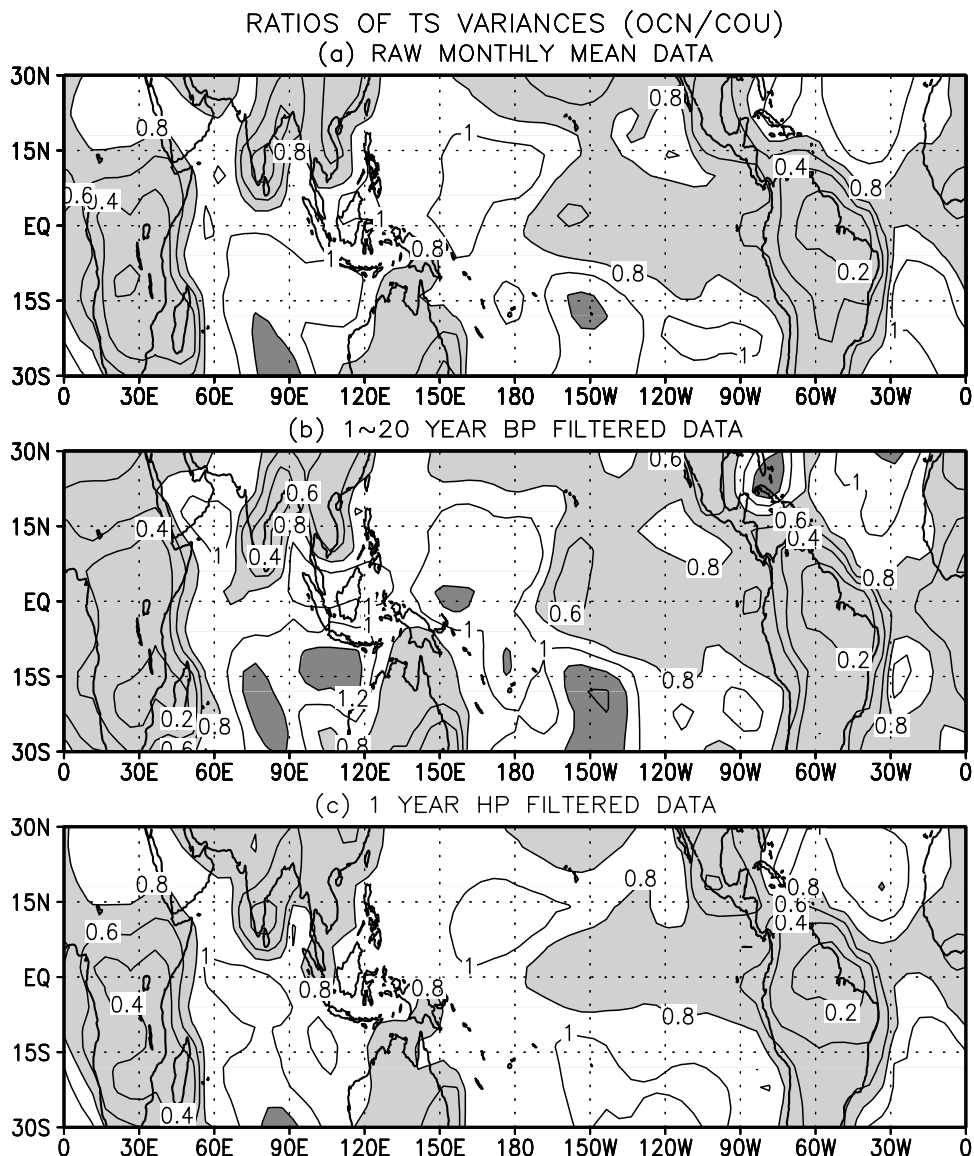


Figure 8. (a) Ratio of OCN/COU surface temperature variances for the raw data, (b) 1–20 year band-pass filter data, (c) and 1 year high-pass filter data. Contour interval is 0.2. The values larger than 1.22 or smaller than 0.82 represent the variance of OCN significant greater (less) than that of COU at the level of 99.9% using an F test.

noise might play a more substantial role in an intermediate model with damped, instead of self-sustained ENSO cycle like the model used in this work.

6.2. Mean State

[26] There are already many investigations demonstrating the influence of mean state changes on the characteristics of ENSO, including its amplitude, structure, major period, and propagation. *Battisti and Hirst* [1989], and *Fedorov and Philander* [2000] indicated that the characteristics of ENSO strongly depend on the background climate state. *Kirtman and Schopf* [1998] found that strong ENSO decades were characterized by higher than normal SST in the central and eastern tropical Pacific and weaker trade winds. With a modified *Zebiak and Cane* [1987] model, *Kirtman and Schopf* [1998] demonstrated that the east-west SST gradient along the tropical Pacific and the wind stress in the central

and eastern tropical Pacific are associated with the amplitude of the SSTA in an ENSO cycle. With the *Zebiak and Cane* [1987] model, *Wang and An* [2002] indicated that the interdecadal variations of the background state, particularly the surface wind and upwelling in the tropical Pacific, affect the properties of ENSO. By modifying model parameterizations, *Codron et al.* [2001] also suggested that a warmer mean state in the tropical eastern Pacific leads to a doubling of the standard deviation of interannual SSTA, to a longer ENSO period, and to a shift from westward propagation to a standing oscillation, which are caused by increasing the sensitivity of the central-west Pacific equatorial wind stress to an eastern Pacific SSTA in the warmer climate and by providing a stronger positive feedback on SSTA. *Arblaster et al.* [2002] showed that a warmer tropical eastern Pacific base state is associated with decreased ENSO variability in the decadal variability context. They found that a deeper

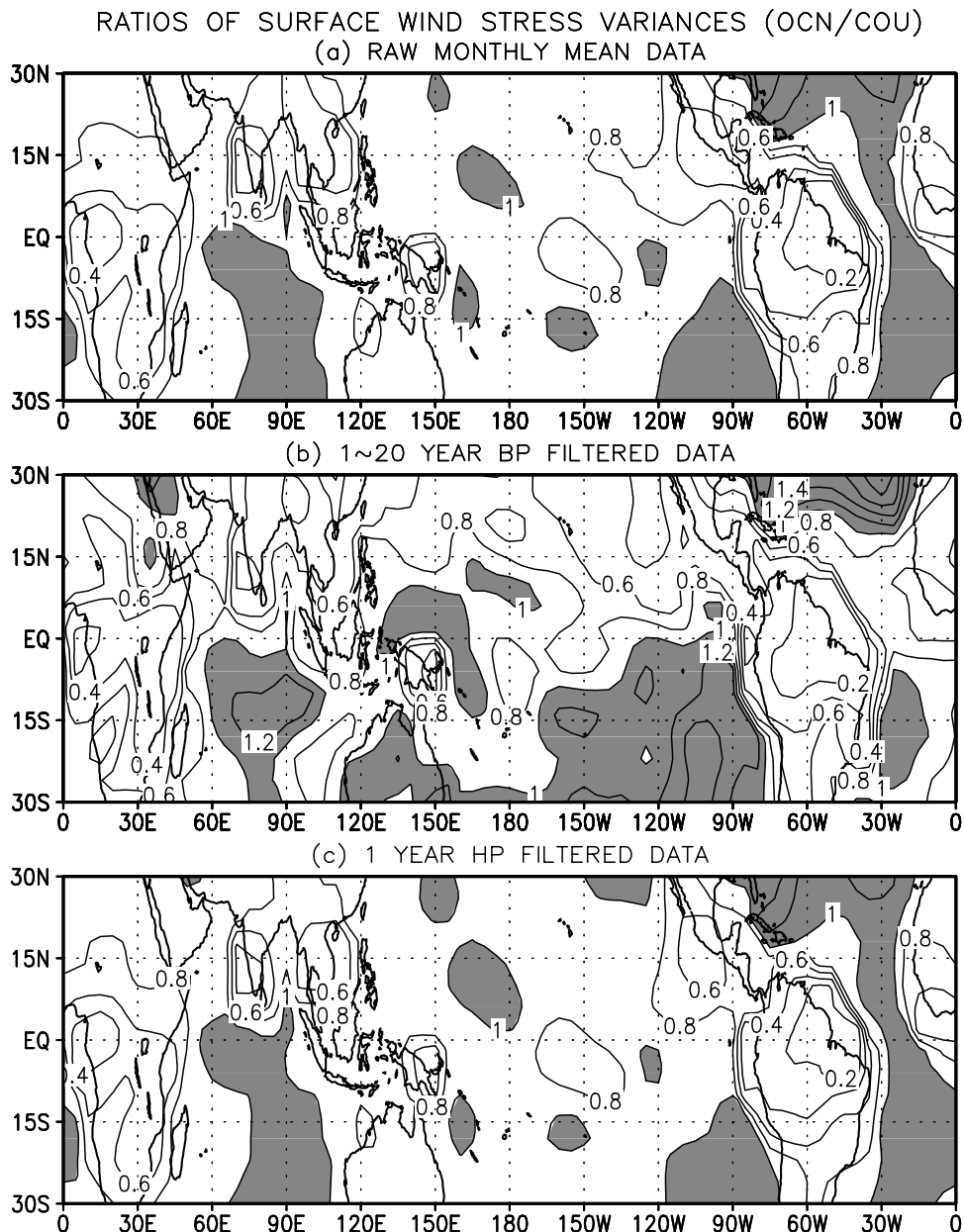


Figure 9. Same as Figure 7, but for the zonal (u) component of surface wind stress. The shaded regions represent ratios larger than 1.0.

thermocline, harder to access cold subthermocline water for a given wind stress fluctuation leads to weaker ENSO.

[27] As in the above subsection we use the intermediate coupled model of *Kirtman and Schopf* [1998] to examine whether the mean state differences between OCN and COU could explain the difference in ENSO variability. This model produces regular ENSO oscillations with a well-defined spectral peak at 5 years in the control run without monthly timescale “atmospheric noise” (Figure 11a). However, when the wind stress anomaly in Figure 5a is added into the wind stress of the control run, following the same procedure as *Kirtman and Schopf* [1998], the model produces a significant suppression of the ENSO variability (Figure 11b) in comparison with the control run (Figure 11a). This suggests a strong connection between the mean wind stress differences in Figure 5a and the

reduction of ENSO variability in Figures 7 and 8. This result indicates that the details of the differences in mean state may be more important than *Kirtman and Schopf* [1998] suggested. Further study indicates that the mean wind stress differences in the eastern tropical Pacific plays a more important role than the wind stress differences elsewhere.

[28] Warming in the eastern tropical Pacific and cooling in the western as shown in Figures 3a, 4a, and 6 result in reduction of the east-west SST gradient along the equator and decrease the ENSO variability. That is consistent with the result of *Arblaster et al.* [2002]. However, according to the previous numerical experiments of *Kirtman and Schopf* [1998] and *Codron et al.* [2001], the gradient reduction is expected to enhance the interannual variability of ENSO [see *Kirtman and Schopf*, 1998, Figures 10 and 11; *Codron*

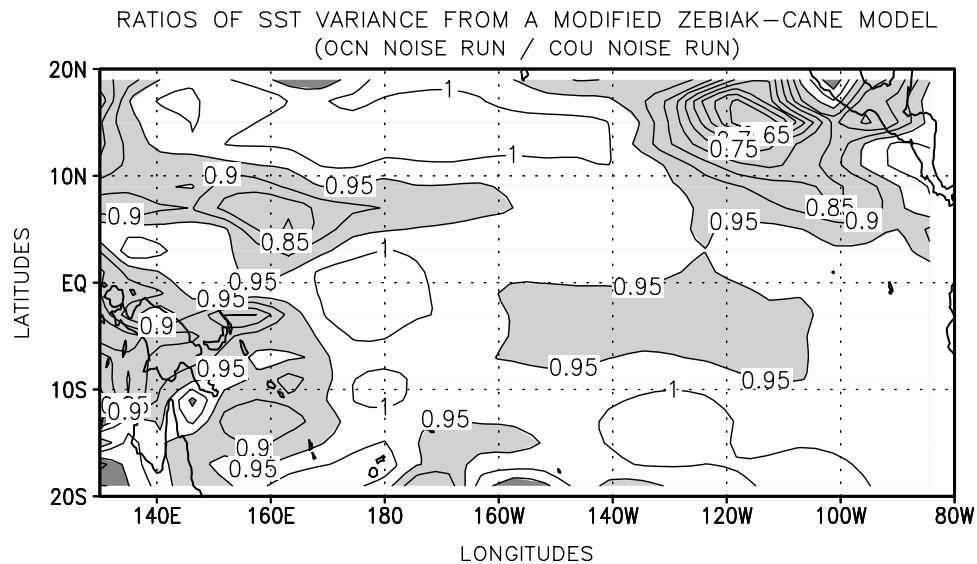


Figure 10. Ratios of the SST variances of the run with OCN atmospheric noise divided by that of the run with COU atmospheric noise. The runs lasted for 82 years with the modified Zebiak and Cane coupled model. Contour interval is 0.05. The shaded regions represent the ratios greater than 1.05 or less than 0.95.

et al., 2001, Figures 6 and 7]. This is clearly not the case of the present work. A possible explanation for the difference between the results of *Kirtman and Schopf* [1998] and the present work in the east-west SST gradient and ENSO variability relationship is that the influence of the cooling over land seems to overcome the effect of the positive SSTA in the eastern tropical Pacific in producing the wind stress anomaly. Thus this cooling might play a role similar to that of negative SSTA in the eastern tropical Pacific. It is also a possibility that changed subsurface equatorial ocean temperature (Figure 6) plays a key role in the ENSO variability change, as discussed by *Arblaster et al.* [2002].

6.3. Sensitivity of Air Sea Coupling

[29] ENSO arises as a result of unstable air-sea interaction, and its amplitude is associated with the sensitivity of air-sea coupling [*Codron et al.*, 2001]. Conceptually, the mean state and atmospheric noise changes in OCN as analyzed in the above subsections cause sensitivity changes, and this results in the ENSO variability changes. Figure 12 shows the sensitivity of equatorial zonal wind stress to Niño3 SSTA in OCN (Figure 12a), COU (Figure 12b), and OCN-COU (Figure 12c). The sensitivity is calculated as the covariance of the wind stress and Niño3 SST divided by the variance of Niño3 SST [*Codron et al.*, 2001].

[30] The sensitivity differences of OCN (Figure 12a) minus COU (Figure 12b) are positive in the central and eastern tropical Pacific and negative in the western (Figure 12c). The differences in the sensitivity imply that for example, given a 1.0C Niño3 SSTA, the OCN simulation has stronger westerly anomalies in the central and eastern tropical Pacific than COU. Conversely, given the same wind stress anomaly in the central and eastern tropical Pacific, the OCN simulation would have a weaker Niño3 SSTA than COU. That means that the Niño3 SST variability becomes less sensitive to the zonal wind stress in OCN than in COU. Thus from the view of sensitivity change, the

Niño3 SST variability would become smaller in OCN than in COU if the wind stress was the same. The westerly anomalies of wind stress of OCN-COU (Figure 5a) further reinforce a weakening in the sensitivity. The connection between wind stress sensitivity and ENSO variability change is supported by the intermediate coupled model experiments discussed in Figure 11.

7. Summary and Discussion

[31] A potential mechanism for the response of ENSO variability to a change in the land surface energy budget was suggested from a comparison of two integrations of the COLA CGCM, a control simulation, in which global soil wetness in the three layers is predicted, and a sensitivity experiment where deep soil moisture is specified leading to the land becoming a net energy sink. The energy sink in the sensitivity experiment was unexpected and should not occur in the physical system. However, the comparison points toward a physically realizable mechanism by which ENSO can refer to changes in land surface properties.

[32] In our simulations, a net energy loss into the land causes cooler land surface in the sensitivity experiment than in the control simulation. The differences over tropical land cause the mean state changes of the coupled system, characterized by a shift in the land/sea partitioning of precipitation toward the oceans, a more westerly wind stress over the tropical Pacific, and a more El Niño-like mean state of the tropical Pacific with a weaker east-west temperature contrast. Meanwhile, as SST variance decreases in the central and eastern tropical Pacific, the ENSO becomes less energetic. However, the ENSO frequencies are not affected significantly.

[33] A series of diagnostic simulations with an intermediate coupled model is used to test the impact of mean state and atmospheric noise changes on the ENSO variability. With the wind stress differences between the two experi-

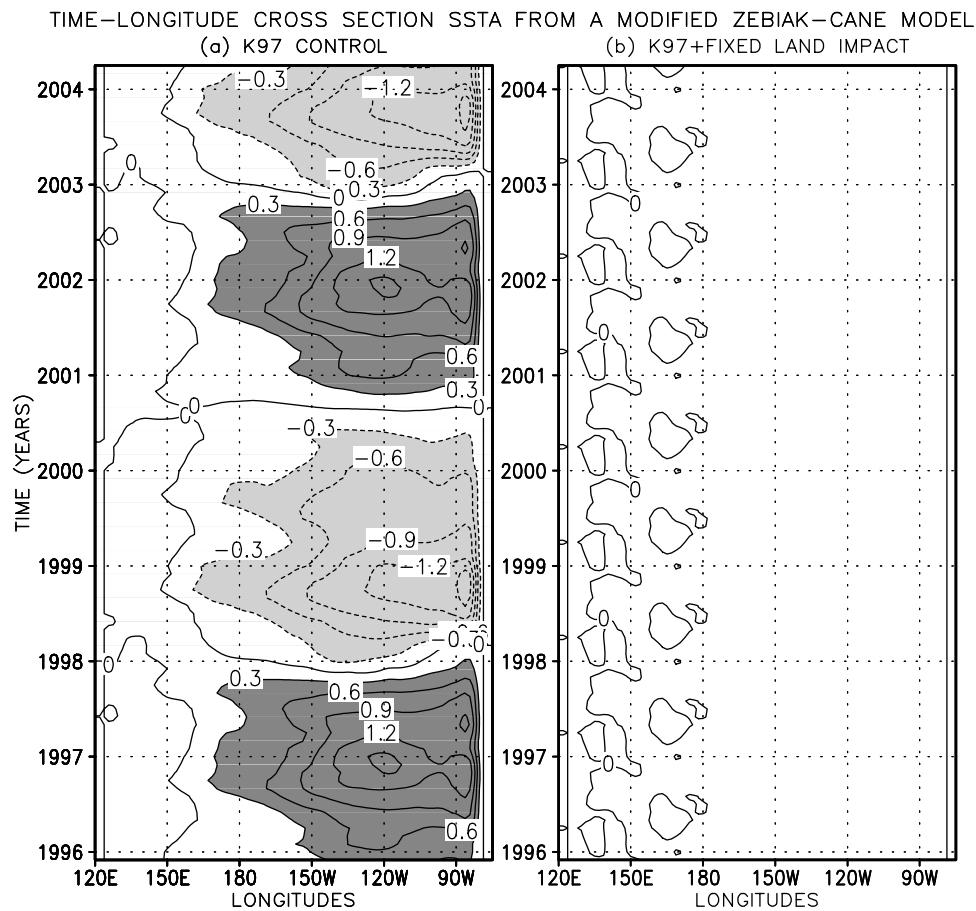


Figure 11. Time-longitude cross section of the SSTA from the modified Zebiak and Cane coupled model simulation with (a) prescribed mean westerlies and (b) with the prescribed mean westerlies plus the wind differences in Figure 4a. Contour interval is 0.3°C . The shaded regions represent SSTA greater than 0.3°C or less than -0.3°C .

ments as input forcing, the model produces a strong decrease of ENSO variance. The model ENSO variance is only slightly impacted by atmospheric noise amplitude changes. This implies that a shift in the mean state and not the change in atmospheric noise amplitude plays a key role in determining the ENSO variance change. In contrast to the control run, the mean state change in the sensitivity experiment favors a reduction in the sensitivity of ENSO variability to surface wind stress, and is consistent with a decrease in ENSO variance. Thus air-sea coupling in the central and eastern tropical Pacific is suppressed, through a change in the mean state of tropical climate.

[34] The study points toward a physically realizable mechanism by which ENSO can be affected by changes in land surface properties. The mechanism is that changes in the land surface properties could lead to changes in the partitioning of the surface energy budget, leading to changes in the local mean surface temperature, moisture, and the convective heating/precipitation distributions. Through atmospheric dynamics, these land changes could then force changes in the distribution of mean surface winds over the equatorial Pacific, changing the mean state of the ocean and the sensitivity of SST to wind stress anomalies, and consequently changing the ENSO variability. In our sensitivity experiment, the sequence is initiated by the unphysical

constraint of fixing the deep soil moisture. However, changing the properties of the land surface in a physically realizable manner (i.e., changing vegetation distribution) could be expected to initiate ENSO changes by the same basic mechanism. Although not demonstrating that the impact of the mechanism is large enough to make it important in the climate system, our experiments provide a framework for understanding the impact of land use changes on ENSO. More physically realistic land surface change experiments with coupled models are necessary to quantify these impacts.

[35] The land-atmosphere interaction in the regions from northern South America to southern North America is directly linked to the changes in the Amazon. Indeed, analogies of the present result can be drawn to the impact of Amazon deforestation on tropical mean climate state and variability. Zeng *et al.* [1996] showed the impact of Amazon deforestation on a change in SST across the Atlantic ocean and in the eastern equatorial Pacific in an intermediate model [Zeng *et al.*, 1996, Figure 13]. In addition, according to the investigation of Nobre *et al.* [1991], there was a significant increase in tropical surface temperature and in subtropical precipitation and a decrease in tropical precipitation when the Amazonian tropical forests were replaced by degraded grass (pasture) in a coupled model of the global

SENSITIVITY OF U COMPONENT OF WIND STRESS TO NINO3 SSTA
(RAW MONTHLY MEAN DATA; DYNES/CM**2/C)

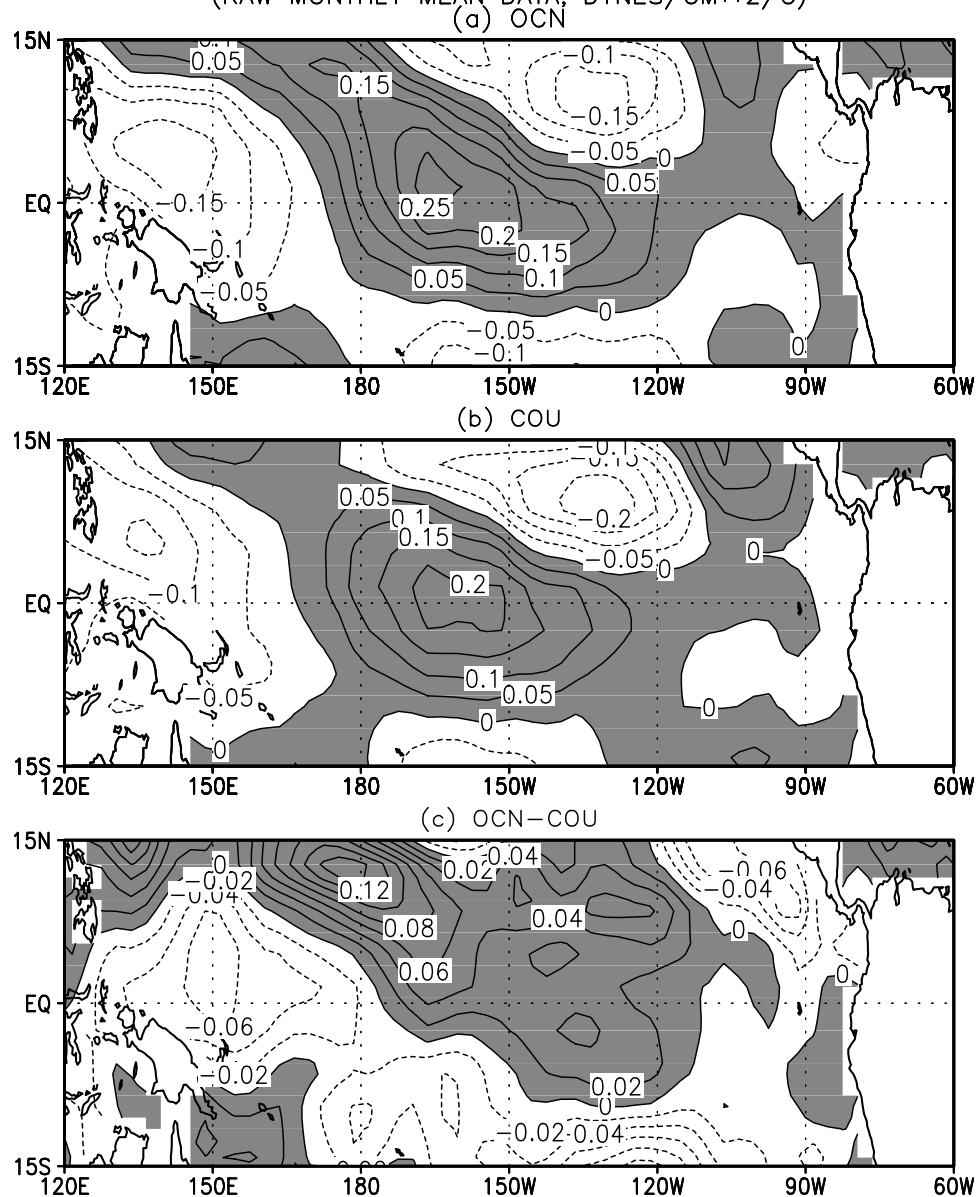


Figure 12. Sensitivity of zonal wind stress to Niño3 index in (a) OCN, (b) COU, and (c) OCN-COU. Contour interval is 0.05 Dynes $(\text{cm } ^\circ\text{C})^{-1}$ in Figures 12a and 12b, and 0.02 Dynes $(\text{cm } ^\circ\text{C})^{-1}$ in Figure 12c. Positive values are shaded. See the text for the definition of sensitivity.

atmosphere and biosphere. On the basis of the conclusion of the present study, cooling (warming) over the Amazon likely results in a reduction (enhancement) of the ENSO variability. Therefore Amazonian deforestation may lead to warming over tropical continents, a precipitation shift from tropical to subtropical land, and consequently an increase in ENSO variability. This suggests potentially important global consequences of Amazonian deforestation and that land surface impact experiments should be performed with coupled models including atmosphere, ocean, and land.

[36] **Acknowledgments.** The authors thank the editor A. Robock and three anonymous reviewers for their suggestions and comments to significantly improve the original manuscript. The authors are indebted to L. Bengtsson, P. Dirneyer, D. Straus, P. Schopf, F-F. Jin, B. Huang, L. Marx, and M. Zhao for their discussion and suggestions. USB is supported

by the Frontier Research System for Global Change through the IARC. This work was supported by grants from the National Science Foundation (ATM 98-14295, ATM 99-07915), the National Oceanic and Atmospheric Administration (NA 96-GP0056), the National Aeronautics and Space Administration (NAG 5-8202), NOAA's CLIVAR Atlantic Program (NA169PI570), and the U. S. Department of Energy (De-FG02-01ER63256).

References

- Arblaster, J. M., G. A. Meehl, and A. M. Moore (2002), Interdecadal modulation of Australian rainfall, *Clim. Dyn.*, *18*, 519–531.
- Barnett, T. P., L. Dumenil, U. Schlese, E. Roeckner, and M. Latif (1989), The effect of Eurasian snow cover on regional and global climate Variations, *J. Atmos. Sci.*, *46*, 661–685.
- Battisti, D. S., and A. C. Hirst (1989), Interannual variability in a tropical atmosphere-ocean model: Influence of the basic state, ocean geometry and nonlinearity, *J. Atmos. Sci.*, *46*, 1687–1712.
- Bhatt, U. S., E. K. Schneider, and D. G. DeWitt (2003), Influence of North American land processes on North Atlantic SST variability, *Global Planet. Change*, *37*, 33–56, doi:10.1016/S0921-8181(02)0190-X.

- Bonan, G. B., D. Pollard, and S. L. Thompson (1992), Effects of boreal forest vegetation on global climate, *Nature*, *359*, 716–718.
- Charney, J., P. Stone, and W. Quirk (1975), Drought in the Sahara: A biogeophysical feedback mechanism, *Science*, *187*, 434–435.
- Chen, D., M. A. Cane, A. Kaplan, S. E. Zebiak, and D. Huang (2004), Predictability of El Niño over the past 148 years, *Nature*, *428*, 733–735, doi:10.1038/nature02439.
- Codron, F., A. Vintzileos, and R. Sadourny (2001), Influence of mean state change on structure of ENSO in tropical coupled GCM, *J. Clim.*, *14*, 730–742.
- Davey, M. K., et al. (2002), STOIC: A study of coupled model climatology and variability in tropical ocean regions, *Clim. Dyn.*, *18*, 403–420.
- Delworth, T. L., and S. Manabe (1988), Influence of potential evaporation on the variabilities of simulated soil wetness and climate, *J. Clim.*, *1*, 523–547.
- Delworth, T. L., and S. Manabe (1989), The influence of soil wetness on near-surface atmosphere variability, *J. Clim.*, *2*, 1447–1462.
- DeWitt, D. G., and E. K. Schneider (1999), On the processes determining the annual cycle of equatorial sea-surface temperature: A coupled general circulation model perspective, *Mon. Weather Rev.*, *127*, 381–395.
- DeWitt, D. G., and E. K. Schneider (2000), The tropical ocean response to a change in solar forcing, *J. Clim.*, *13*, 1133–1149.
- Dickinson, R., and A. Henderson-Sellers (1988), Modeling tropical Deforestation—A study of GCM land surface parameterizations, *Q. J. R. Meteorol. Soc.*, *114*, 439–462.
- Dirmeyer, P. A., and F. J. Zeng (1997), A two-dimensional implementation of the Simple Biosphere (SiB) model, *COLA Rep.* *48*, 30 pp., Cent. for Ocean Land Atmos. Stud., Calverton, Md.
- Fedorov, A. V., and S. G. Philander (2000), Is El Niño changing?, *Science*, *288*, 1997–2002.
- Flügel, M., and P. Chang (1996), Impact of dynamical and stochastic processes on the predictability of ENSO, *Geophys. Res. Lett.*, *23*, 2089–2092.
- Gedney, N., and P. J. Valdes (2000), The effect of Amazonian deforestation on the Northern Hemisphere circulation and climate, *Geophys. Res. Lett.*, *27*, 3053–3056.
- Kalnay, E., et al. (1996), The NCEP/NCAR 40-year reanalysis Project, *Bull. Am. Meteorol. Soc.*, *77*, 437–471.
- Kirtman, B. P. (1997), Oceanic Rossby wave dynamics and the ENSO period in a coupled model, *J. Clim.*, *10*, 1690–1704.
- Kirtman, B. P., and P. S. Schopf (1998), Decadal variability in ENSO predictability and prediction, *J. Clim.*, *11*, 2804–2822.
- Kirtman, B. P., and J. Shukla (2002), Interactive coupled ensemble: A new coupling strategy for CGCMs, *Geophys. Res. Lett.*, *29*(10), 1367, doi:10.1029/2002GL014834.
- Kleeman, R., and A. M. Moore (1997), A theory for the limitation of ENSO predictability due to stochastic atmospheric transients, *J. Atmos. Sci.*, *54*, 753–767.
- Kleeman, R., and S. B. Power (1994), Limits to predictability in a coupled ocean-atmosphere model due to atmospheric noise, *Tellus, Ser. A*, *46*, 529–540.
- Latif, M., et al. (2001), ENSIP: The El Niño simulation intercomparison project, *Clim. Dyn.*, *18*, 255–276.
- Meehl, G. A. (1994), Influence of the land surface in the Asian summer monsoon: External conditions versus internal feedbacks, *J. Clim.*, *7*, 1033–1049.
- Meehl, G. A. (1997), The south Asian monsoon and the tropospheric biennial Oscillation, *J. Clim.*, *10*, 1921–1943.
- Nobre, C. A., P. J. Sellers, and J. Shukla (1991), Amazonian deforestation and regional climate change, *J. Clim.*, *4*, 957–988.
- Press, W. T., S. A. Teukolsky, W. T. Vetterling, and B. P. Flannery (1992), *Numerical Recipes in Fortran, The Art of Scientific Computing*, 2nd ed., 963 pp., Cambridge Univ. Press, New York.
- Rasmusson, E. M., and T. H. Carpenter (1982), Variations in tropical sea surface temperature and surface wind fields associated with the Southern Oscillation and El Niño, *Mon. Weather Rev.*, *110*, 354–384.
- Schneider, E. K. (2001), The causes of differences between equatorial Pacific SST simulations of two coupled ocean-atmosphere general circulation models, *J. Clim.*, *15*, 449–469.
- Schneider, E. K., and J. L. Kinter III (1994), An examination of internally generated variability in long climate simulations, *Clim. Dyn.*, *10*, 181–204.
- Sellers, P. J., Y. Mintz, Y. C. Sud, and A. Dalcher (1986), A simple biosphere model (SiB) for use within general circulation models, *J. Atmos. Sci.*, *43*, 505–531.
- Shukla, J., and Y. Mintz (1982), The influence of land-surface evapotranspiration on Earth's climate, *Science*, *215*, 1498–1501.
- Thompson, C. J., and D. S. Battisti (2001), A linear stochastic dynamical model of ENSO. Part II: Analysis, *J. Clim.*, *14*, 445–466.
- Wajsoiwicz, R. C., and E. K. Schneider (2001), The Indonesian through-flow's effect on global climate determined from the COLA coupled climate system, *J. Clim.*, *14*, 3029–3042.
- Wang, B., and S. I. An (2002), A mechanism for decadal changes of ENSO behavior: Roles of background wind changes, *Clim. Dyn.*, *18*, 475–486.
- Xue, Y., and J. Shukla (1993), The influence of land-surface properties on Sahel climate. 1. Desertification, *J. Clim.*, *6*, 2232–2245.
- Xue, Y., P. J. Sellers, J. L. Kinter, and J. Shukla (1991), A simplified biosphere model for global climate studies, *J. Clim.*, *4*, 345–364.
- Xue, Y., F. J. Zeng, and C. A. Schlosser (1996), SSiB and its sensitivity to soil properties – A case study using HAPEX-Mobihy data, *Global Planet. Change*, *13*, 183–194.
- Yasunari, T., A. Kitoh, and T. Tokioka (1991), Local and remote responses to excessive snow mass over Eurasia appearing in the northern spring and summer climate, *J. Meteorol. Soc. Jpn.*, *69*, 473–487.
- Zebiak, S. E. (1989), On the 30–60 day oscillation and the prediction of El Niño, *J. Clim.*, *2*, 1381–1387.
- Zebiak, S. E., and M. A. Cane (1987), A model of El Niño and the Southern Oscillation, *Mon. Weather Rev.*, *115*, 2262–2278.
- Zeng, N., and J. D. Neelin (1999), A land-atmosphere interaction theory for the tropical deforestation problem, *J. Clim.*, *12*, 857–872.
- Zeng, N., R. E. Dickinson, and X. Zeng (1996), Climatic impact of Amazon deforestation—A mechanistic model study, *J. Clim.*, *9*, 859–883.
- Zhang, H., K. McGuffie, and A. Henderson-Sellers (1996), Impacts of tropical deforestation. Part II: The role of large-scale dynamics, *J. Clim.*, *9*, 2498–2521.
- Zhao, M., and A. J. Pitman (2002), The impact of land cover change and increasing carbon dioxide on the extreme and frequency of maximum temperature and convective precipitation, *Geophys. Res. Lett.*, *29*(6), 1078, doi:10.1029/2001GL013476.

U. S. Bhatt, International Arctic Research Center, Frontier Research System for Global Change, University of Alaska Fairbanks, 930 Koyukuk Dr., P. O. Box 75-7335, Fairbanks, AK 99775, USA.

Z.-Z. Hu, B. P. Kirtman, and E. K. Schneider, Center for Ocean-Land-Atmosphere Studies, 4041 Powder Mill Rd., Suite 302, Calverton, MD 20705, USA. (hu@cola.iges.org)